Journal of Molecular Structure 1252 (2022) 132141

Contents lists available at ScienceDirect

Journal of Molecular Structure

journal homepage: www.elsevier.com/locate/molstr

Effect of pH on the structure and stability of irisin, a multifunctional protein: Multispectroscopic and molecular dynamics simulation approach

Rashid Waseem[a], Anas Shamsi[a], Mohd Shahbaz[b,c], Tanzeel Khan[a], Syed Naqui Kazim[a], Faizan Ahmad[a], Md. Imtaiyaz Hassan[a], Asimul Islam[a,*]

[a] Centre for Interdisciplinary Research in Basic Sciences, Jamia Millia Islamia, Jamia Nagar, New Delhi 110025, India
[b] South African Medical Research Council Bioinformatics Unit, South African National Bioinformatics Institute, University of the Western Cape, Private Bag X17, Bellville, Cape Town 7535, South Africa
[c] Laboratory of Computational Modeling of Drugs, South Ural State University, 76 Lenin prospekt, Chelyabinsk 454080, Russia

ARTICLE INFO

Article history:
Received 7 October 2021
Revised 26 November 2021
Accepted 7 December 2021
Available online 10 December 2021

Keywords:
Irisin
Structure-function relationships
Molecular dynamic simulation

ABSTRACT

Irisin is a potential therapeutic agent to prevent or treat various metabolic-related disorders and neurodegenerative diseases viz. Alzheimer's disease (AD). In this study, we have employed a multispectroscopic approach to elucidate the structural and conformational changes in the irisin at varying pH (pH 2.0 to 12.0). The spectroscopic measurements revealed that irisin maintains its structure (both secondary and tertiary) in the alkaline pH range, with minimal structural changes observed across it. However, secondary and tertiary structural alterations were evident across the acidic pH range. CD spectroscopy suggested a gain of the secondary structure in the acidic pH range, implying that irisin is more stable at acidic pH, with maximum stability and compactness observed at pH 4.0. *In vitro* observations were further validated by *in silico* studies. Molecular dynamics simulation also suggested that irisin assumes higher stability in the conformational space at pH 4.0 and 6.0 than the rest of the system. This study can serve as a platform to delineate the enhanced functionality of irisin at lower pH that can be implicated in developing therapies for metabolic disorders, including diabetes and obesity.

1. Introduction

Physical exercise is known to have several beneficial effects on the body. These beneficial effects have been attributed to various cytokines and metabolites that mediate the systemic benefits of exercise [1]. Irisin is one of these cytokines which is secreted by myocytes during or immediately after exercise. Irisin, a fragment of transmembrane protein fibronectin type III domain containing 5 (FNDC5), reprograms adipose tissue metabolism by inducing changes in adipose tissue through thermogenesis activation [2]. Irisin converts white adipocytes into brown adipocytes by upregulating the expression of uncoupling protein 1 (UCP1) through activation of ERK and p38 MAPK signaling [2]. Irisin also enhances sensitivity to insulin by increasing glycogenesis and reducing gluconeogenesis and therefore acts as an insulin-sensitizing hormone [3]. These properties of irisin make it a potential therapeutic agent for metabolic disorders, including obesity and diabetes.

A recent investigation revealed some important biological functions of irisin in the nervous system [4] and bone metabolism [5]. It was established that irisin activates the Akt and ERK1/2 signaling pathways in brain tissues and contributes to the neuroprotective effects of physical exercise in cerebral ischemia. Hence, it is a promising agent for the prevention and treatment of ischemic stroke [6]. Irisin also shows protective action against the aberrant expression of synapse-related genes, thereby signifying its role in attenuating synaptic and memory impairments in AD mouse models [4]. Therefore, enhancing brain FNDC5/irisin levels can be a novel therapeutic strategy to protect and/or repair synapse function or prevent memory impairment in AD [4].

Moreover, irisin also targets bone tissues and positively affects cortical mineral density and improves bone strength as well as geometry in mice [5]. Irisin has a role in osteoblast proliferation, and it can protect osteocytes against apoptosis in culture and upregulates the expression of sclerostin, a key regulator of bone remodeling, *in vivo* [7]. Irisin is also involved in carcinogenesis, although

Abbreviations: AD, Alzheimer's disease; FNDC5, Fibronectin type 3 domain containing protein 5; UCP1, Uncoupling protein 1; MAPK, Mitogen activated protein kinase; CD, Circular dichroism; MD, Molecular dynamics; PMSF, Phenylmethylsulfonyl fluoride; ERK, Extracellular-signal-regulated kinase.

* Corresponding author.
E-mail address: aislam@jmi.ac.in (A. Islam).

https://doi.org/10.1016/j.molstruc.2021.132141
0022-2860/

its role in cancer progression is uncertain [8]. Most of the available data now favor irisin as a potential substance for cancer regression by reducing pro-inflammatory markers linked to obesity [9,10]. Still, further research is needed to understand the involvement of irisin in cancer prevention and therapeutics.

Irisin is a cleaved portion of a cell membrane protein called fibronectin type III domain-containing protein 5 (FNDC5/FRCP2/PeP) [11]. FNDC5 comprises of a signal peptide, a fibronectin III domain and a hydrophobic C-terminal domain. FNDC5 is a 209 amino acids residue protein with an N-terminal 29-residue signal sequence, followed by a putative fibronectin III (FNIII) 2 domain (94 aa), a linking peptide (28 aa), a transmembrane domain (19 aa), and a 39-residue cytoplasmic domain. The mature peptide of irisin, a proteolytically cleaved portion of FNDC5, is of 112 amino acids (32–143 amino acids of FNDC5). The molecular mass of irisin as a monomer is predicted to be 12 kDa [2]. Irisin undergoes glycosylation at two arginine residues and dimerizes, increasing its molecular weight to 20–32 kDa depending on the number and structure of oligosaccharides (glycans) attached to the protein molecule during the post-translational process of N-glycosylation [2]. The irisin crystal structure suggests that this protein has an antiparallel β-pleated sheet shared by the monomers coupled by 10 hydrogen bonds between the four ribbons on each side, which provides stability to protein [12]. Irisin is a stable protein whose melting temperature (T_m) is 72 °C [13]. The receptor of irisin has not been identified. However, recently it was found that the αV family of integrin receptors is likely to be the irisin receptors in osteocyte and thermogenic fats [7].

Various factors influence the structure and stability of proteins, in which pH is of utmost importance. In proteins, the pH of the solvent determines the ionization state of the side chain of amino acids. These amino acids are involved in electrostatic interactions, which are required for proper conformation and stable structure of proteins. Change in pH causes protonation or deprotonation of those ionizable groups, which can alter the charge pattern and disrupt electrostatic interactions, leading to the unfolding or denaturation of proteins. In this work, we have investigated the effect of pH on the structure and stability of irisin using various spectroscopic techniques. Different spectroscopic tools are being used to study amino acid structures to understand the molecular structure of proteins [14–16]. For this, we have employed circular dichroism (CD), absorbance and fluorescence measurements at different pH values (2.0–12.0). Various molecular modeling tools are available to acquire the molecular structure of proteins and complement the spectroscopic results [17,18]. Therefore, we have studied conformational dynamics of the protein using classical molecular dynamics (MD) simulation to elucidate the structural changes taking place in irisin at different pH values.

2. Material and methods

2.1. Materials

The expression construct of irisin (pET15b-His-3C-irisin) was purchased from Addgene (122612). Ni-NTA resin for protein purification was purchased from Genetix (Bangalore, India). Tris–HCl was purchased from Sigma Aldrich (USA). DH5α cells and C41-DE3 cells were purchased from the Invitrogen (USA). Luria agar and Luria Bertani broth for bacterial culture were purchased from Himedia (India). Ampicillin was obtained from MP Biomedicals, LLC (France). IPTG was purchased from Sisco Research Laboratories.

2.2. Expression and purification

The irisin was expressed, and the protein was purified using standard procedure [12,19]. In brief, transformed E. coli C41 (DE3) cells were grown, and 0.5 mM IPTG was added to induce irisin expression. Cultures were harvested and dissolved in lysis buffer (50 mM Tris–HCl buffer, pH 7.5, containing 300 mM NaCl, 5% (v/v) glycerol, 0.5 mM β-mercaptoethanol, and 1 mM phenyl methane sulfonyl fluoride (PMSF). The obtained supernatant was loaded on equilibrated Ni–NTA column and the bound protein was eluted with 150 mM imidazole. The fractions of eluted irisin protein were collected and checked for purity on SDS-PAGE.

2.3. Sample preparation

Aliquots of irisin were prepared at different pH. Buffers used for the experiment were as follows: pH 2.0 (glycine-HCl), pH 4.0 (sodium acetate), pH 6.0 (sodium phosphate), pH 7.5, 8.0 (Tris–HCl), pH 10.0, 12.0 (Glycine-NaOH). The protein samples were incubated at 25 °C for 6 h before carrying out spectroscopic measurements. To obtain accurate results, three replicates were analyzed for each set.

2.4. Circular dichroism (CD) measurement

Circular dichroism (CD) experiment was carried out on Jasco spectropolarimeter (model J-1500) equipped with a Peltier type temperature controller. Far-UV CD spectra of irisin samples at different pH (2.0–12.0) were recorded at 25 ± 0.1 °C using a cuvette of 1 mm path length cell and protein concentration of 15 µM. Spectra were recorded in the far-UV range (200–250 nm) with a scan speed of 100 nm/min and a response time of 1 s [20]. The results were expressed as mean residue ellipticity (MRE) in deg cm^2 dmol^{-1} which is defined as:

$$\mathrm{MRE} = \mathrm{MRW} \times \theta_{observed}/10 \times l \times c \quad (1)$$

where $\theta_{observed}$ is the observed ellipticity in milli degrees, MRW is the mean residue weight of the protein, l being the path length in cm and c being the protein concentration in mg/ml Eq. (1).

2.4.1. Estimation of secondary structure from far-UV CD spectra

We have calculated the secondary structural content of irisin using the Eq. (2) where the observed mean residue ellipticity ($[\theta]_\lambda{}^{\mathrm{p}}$) of the protein is related as the linear combination of all structures, i.e.,

$$[\theta]_\lambda{}^{\mathrm{p}} = \mathrm{f}_\alpha[\theta]_\lambda{}^{\alpha} + \mathrm{f}_\beta[\theta]_\lambda{}^{\beta} + \mathrm{f_t}[\theta]_\lambda{}^{\mathrm{t}} + \mathrm{fr}[\theta]_\lambda{}^{\mathrm{r}} \quad (2)$$

where f_α,f_β,$\mathrm{f_t}$ and fr are the fractions of α-helix, β-sheet, turn and random coil, respectively, and $[\theta]_\lambda{}^{\alpha}$, $[\theta]_\lambda{}^{\beta}$, $[\theta]_\lambda{}^{\mathrm{t}}$ and $[\theta]_\lambda{}^{\mathrm{r}}$ are the mean residues ellipticities of pure α-helix, β-sheet, β-turn and random coil at wavelength λ, respectively. Due to the uncertainty of $[\theta]_\lambda{}^{\mathrm{t}}$ of proteins and inaccessibility of measurements beyond 210 nm, Eq. (2) was reduced to the following form,

$$[\theta]_\lambda{}^{\mathrm{p}} = \mathrm{f}_\alpha[\theta]_\lambda{}^{\alpha} + \mathrm{f}_\beta[\theta]_\lambda{}^{\beta} + \mathrm{fr}[\theta]_\lambda{}^{\mathrm{R}} \quad (3)$$

where R represent structures which is not the part of α-helix and β sheet. Using data provided by Yang et al. [21] for the reference spectra, we analysed each CD curve of the native protein for the elements of secondary structure according to Eq. (3).

2.5. Fluorescence measurements

Fluorescence spectra were measured in Jasco spectrofluorometer (FP-6200) in quartz cuvette of path length 1 mm at 25 ± 0.1 °C, maintained by an external thermostatic water circulator, with both excitation and emission slit width set at 10 nm.. The excitation wavelength was set at 280 nm, and emission spectra were recorded in the wavelength region 300–400 nm. The concentration of irisin in each sample was 4 µM. All the measurements were carried out in triplicates and reported spectra were taken after subtracting appropriate blanks.

2.6. UV spectroscopic measurements

JASCO UV-660 UV/Vis spectrophotometer, whose temperature was maintained by circulating water from an external refrigerated water bath, was used to record UV spectra of irisin samples at varying pH (2.0–12.0). The protein concentration in each sample was 10 μM. All measurements were carried out using a 1 cm path length cuvette in the 240–340 nm wavelength range. All the spectra were taken in triplicates, and their average was used for calculation.

2.7. Molecular dynamic (MD) simulations

During MD simulation study at a particular pH, the solvent conditions of the protein system are generally modeled by changing the protonation state of the titrable residues using the pKa values, which can be calculated by various available methods [22,23]. In the present study, the pKa values were calculated using the H++ server [24], and the protonation values were adjusted based on the magnitude of the pH (from 2.0 to 12.0) in the structure of the irisin protein (PDB ID - 4LSD). On the basis of the variations in the pKa values, the protonation and deprotonation of the titrable residues were performed. The modified protonated forms of the irisin protein were subjected to MD simulations using GROMACS 2018–2 package; a free and open-source software [25]. The topology of irisin protein at different pH conditions was generated using AMBER ff99SB [26], and solvation was performed using SPC/E water model [27]. The solvated systems of irisin protein were neutralized by adding a suitable number of Na^+ and Cl^- counterions.

Consequently, the generated systems were minimized using the steepest descent algorithm in GROMACS with a convergence criterion of 0.005 kcal/mol. The equilibration stage was performed separately in NVT (constant volume) and NPT (constant pressure) ensemble conditions, each at 1 ns time scale. The temperature and pressure were maintained at 300 K and 1 bar during the equilibration step using Berendsen weak coupling method and Parrinello-Rahman barostat. The final production stage of MD simulations was performed using the LINCS algorithm for 100 ns timescale, and trajectories were generated, which were analyzed to understand the changes in the conformational behavior of irisin in different studied pH conditions. The variations in the structural patterns were observed in terms of changes in values of root mean dquare deviations (RMSD), radius of gyration (R_g). At the same time, the free energy associated parameters were analyzed by performing the eigen vector projections and free energy landscape calculations.

3. Results and discussion

3.1. Expression and purification of recombinant irisin

The expression construct of irisin (pET15b-His-3C-irisin) was transformed into E. coli C41 (DE3) cells. Transformed cells were grown, and 0.5 mM IPTG was used to induce irisin expression. The protein was purified under native conditions using Ni-NTA affinity column chromatography, and a single band of approximately 15–16 kDa was observed on SDS-PAGE (Fig. S1).

3.2. Far-UV CD measurements

To see the effect of pH on the secondary structure of irisin, CD spectroscopy was employed. The crystal structure of irisin suggests it to be a β-sheet rich protein (PDB ID- 4LSD). Far-UV CD spectra of irisin in different pH conditions have been shown in Fig. 1. At pH 7.5, a negative peak at 217 nm indicates it to be a β-sheet structure, which is in excellent agreement with the crystal structure of irisin. The far-UV CD spectra of irisin in the acidic pH range (pH 2.0–6.0) are shown in Fig. 1A, where a remarkable increase in the secondary structure was observed. On the other hand, Far-UV CD spectra of irisin were almost similar in the alkaline pH range (pH 7.5–12) with no peak shift except for pH 12.0, where a slight peak shift coupled with an increase in dichroic signal was evident (Fig. 1B). Secondary structure estimation was also carried out at various pH. Each CD spectrum was analysed for the content of secondary structure using the software developed by Yang et al. [21] and the results of these analyses are shown in Table-1. It was found that as we move towards acidic pH, there was an increase in the β-sheet content, with maximum β-sheet structure obtained at pH 2.0. (Table 1). There are no significant differences in the CD spectra in the alkaline pH range (pH 7.5–12.0), implying that pH does not affect the overall secondary structure in this range, with irisin retaining its secondary structure. This was further confirmed by estimating β-sheet content of irisin in the alkaline pH range and no significant change was observed. These observations signify that minimal secondary structural perturbations occur in the alkaline pH range while secondary structural changes are more evident in the acidic pH range, with maximum secondary structure observed at pH 2.0. It cannot be expected that these methods of secondary structure estimation always give accurate results, but the general trend may be correct. It is important to note that the content of aromatic amino acids makes the analysis of the data in the far-UV region difficult and could have influenced the accuracy of the secondary structure determination [28].

Table 1
Estimated β-sheet structural content of irisin at various pH using secondary structural prediction software provided with Jasco J1500 CD spectrophotometer.

pH	β-sheet (%)
2.0	52.0%
4.0	46.2%
6.0	40.4%
7.5	38.0%
8.0	38.4%
10.0	39.2%
12.0	41.5%

3.3. Fluorescence measurements

Intrinsic fluorescence studies were carried out to see the effect of pH on the tertiary structure of irisin. Since intrinsic fluorescence of proteins depends on the environment of aromatic amino acid residues [29,30], a change in intrinsic fluorescence is a sign of change in the local environment of aromatic amino acid residues. Therefore, we employed fluorescence measurement to study the effect of pH on irisin structure and structural changes depicted from the emission spectrum. Irisin consists of one tyrosine and two tryptophan residues; Trp51, Trp90 and Tyr98. Trp90 is exposed and is accessible to solvent while Trp51 and Tyr98 are buried. Irisin showed emission maxima at 344 nm at pH 7.5 (Fig. 2A and B). Fig. 2A shows the fluorescence emission spectra of irisin in the pH range of 7.5–2.0. In the acidic pH range (7.5–2.0), a marked blue shift was observed along with a considerable decrease in fluorescence intensity, with a significant blue shift of 7 nm and 9 nm at pH 4.0 and pH 2.0 respectively. The decrease in fluorescence intensity coupled with blueshift is implicative that pH-induced structural changes are taking place in irisin in the acidic pH range. Fig. 2B shows the fluorescence emission spectra of irisin in the pH range of 7.5–12.0. In the alkaline pH range (pH 7.5–12.0), no

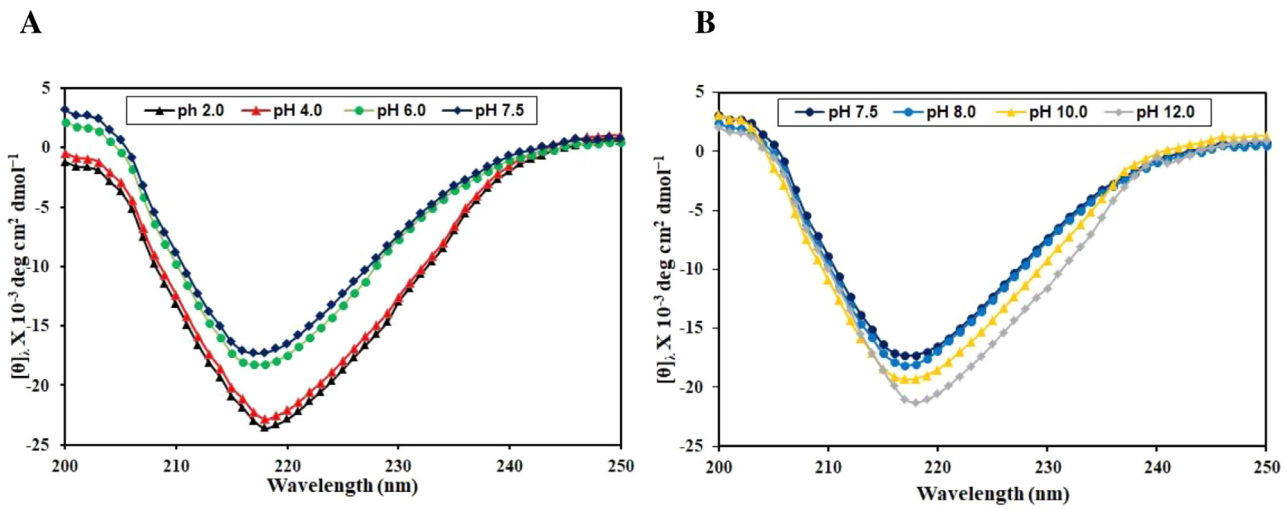

Fig. 1. (A) CD spectra of irisin under acidic pH conditions (B) CD spectra of irisin under alkaline pH conditions.

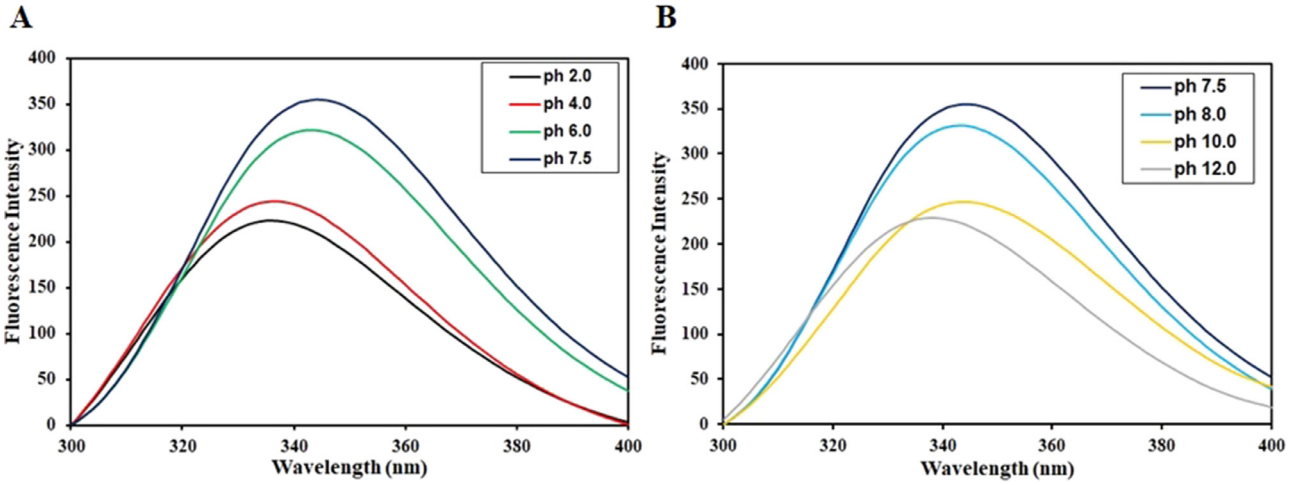

Fig. 2. (A) Fluorescence spectra of irisin under acidic pH conditions (B) Fluorescence spectra of irisin under alkaline pH conditions.

shift in the emission maxima was observed, implying no significant structural alterations taking place in irisin in this pH range. A decrease in fluorescence intensity was attributable to self-quenching or deprotonation of neighboring basic amino acids. At pH 12.0, a blue shift of 6 nm was observed with decreased fluorescence intensity that might be due to the conformational change in protein at extreme pH caused by disruption of electrostatic interaction and ionization of tryptophan residue [31].

These findings are in line with CD observations affirming that minimal structural alterations occur in the alkaline pH range whilst changes in the secondary and tertiary structure take place in the acidic pH range.

3.4. UV–vis absorption measurements

Near-UV absorption is a sensitive probe to study the environment of aromatic amino acid residues like tyrosine and tryptophan. To further examine the effect of pH on the tertiary structure of irisin, UV–vis spectroscopy was employed (240–340 nm). Fig. 3A shows absorption spectra of irisin in the acidic pH range (2.0–7.5). As we decrease pH from 7.5 to 2.0, a slight decrease in absorption was observed in absorption spectra, suggesting that irisin is in a more compact state. While in the alkaline pH range (7.5–12), no significant changes were observed in UV spectra (Fig. 3B). A remarkable decrease in absorbance was observed at pH below 7.5. This result is in line with the observation found in fluorescence and CD measurement, which suggests that the tertiary structure of irisin is more stable in the acidic pH range. We have already reported the thermal denaturation study of irisin though UV melting at 280 nm and T_m obtained at pH 7.5 is 72 °C [13].

3.5. Molecular dynamics (MD) simulations

The effect of diverse pH conditions on the conformational behavior of irisin was analyzed, and the generated outcomes were compared and validated the experimental findings. The changes in the compactness of the irisin protein in different pH conditions were assessed in terms of the radius of gyration. The irisin assumes higher compactness in between pH 2.0 and 6.0 as compared to the pH 7.5, pH 10.0 and pH 12.0, which is evident from the projected R_g values which were observed between 1.35 and 1.4 nm, particularly the R_g values for pH > 7.5 showed sharp continuous elevated fluctuations during 100 ns MD simulations (Fig. 4). This behavior may be attributed to developing a more compact and stable conformation state between pH 2.0 and 6.0. On the contrary, sharp changes were observed in RMSD values with pH 6.0 to 12.0 fluctuated between 0.2 and 0.3 nm, while the RMSD values for pH 4.0 were observed below 0.1 nm (Fig. 5). These observations indicated that the irisin protein became more stable at pH 4.0 than the other studied systems. The flexible nature of the studied sys-

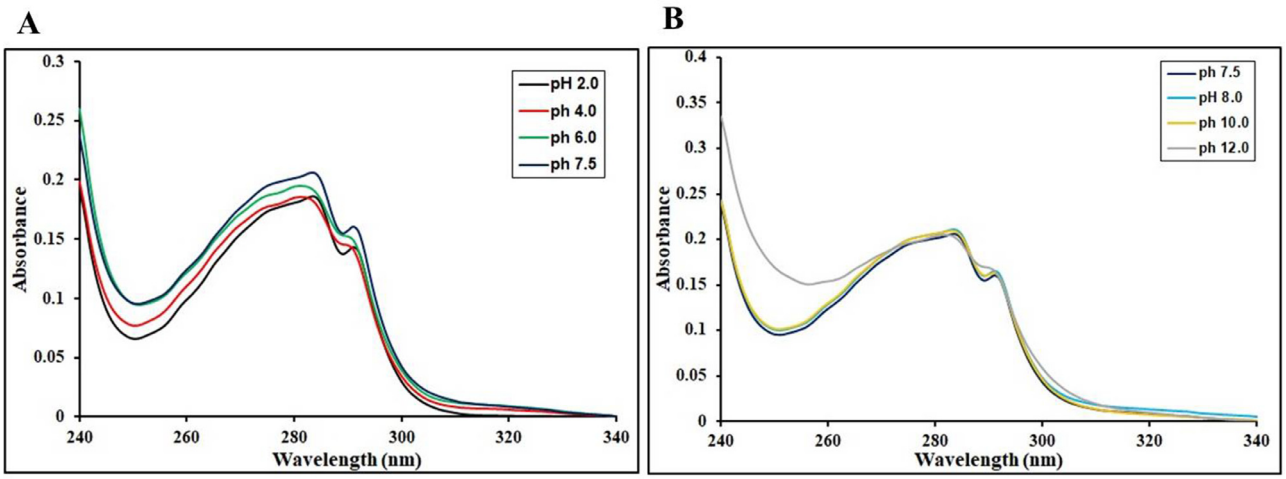

Fig. 3. (A) Absorption spectra of irisin under acidic pH conditions (B) Absorption spectra of irisin under alkaline pH conditions.

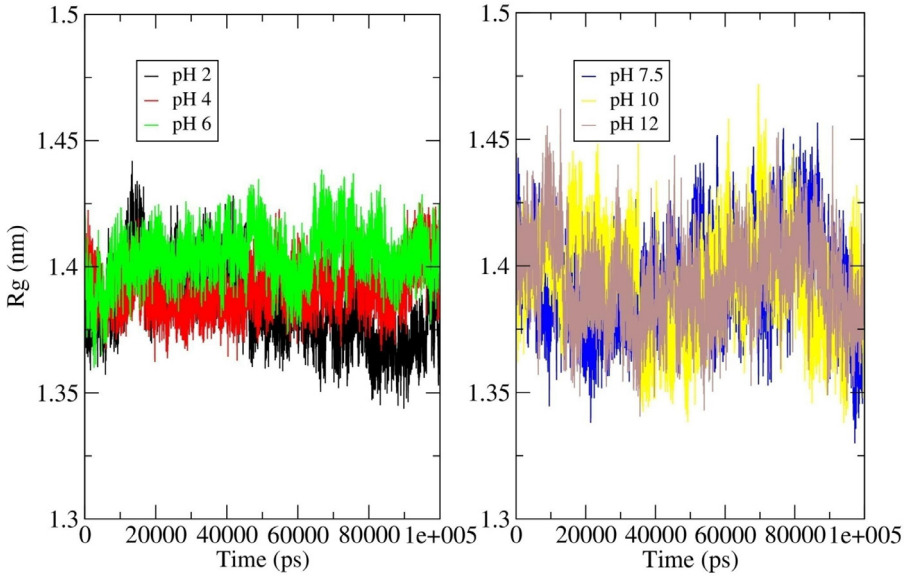

Fig. 4. The R_g curves showing the variations in the structural compactness of the irisin at different pH values (A) Acidic Range and (B) Alkaline range.

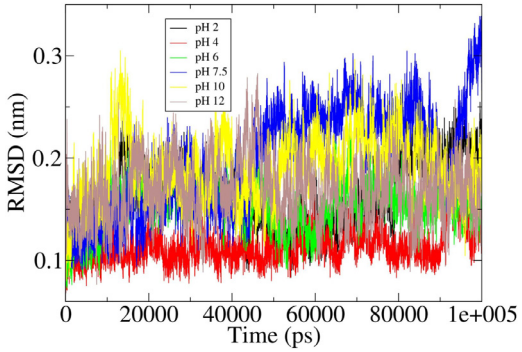

Fig. 5. The RMSD plots highlighting the changes between the stabilities in the observed systems.

tems was evaluated using the 2-D eigenvector projections, which showed the highest flexibility between pH 7.5 and pH 12 while a compact structure was observed for pH 4.0 and pH 6.0, as a result of lesser flexibility in the respective conditions, a relatively higher folding state is attained than rest of the systems (Fig. 6). Moreover, the free energy landscapes showed higher energy-based stability for pH 4 - pH 6, with structures slightly perturbed in range of pH 7.5 - pH 12.0 (Fig. 7). These observations indicated that the irisin assumed higher stability in the conformational space in pH 4.0 and 6.0 than the rest of the system, resulting in higher compactness and folding state in the respective acidic conditions.

3.6. pH dependence and the net charge on protein stability

The net charge on protein has a vital role in protein stability, solubility and activity at any given pH. The net charge on protein at any given pH is mainly determined by the number of ionizable groups and pK values (pKs) of the ionizable groups [32]. The net charge on any protein is zero at its isoelectric point (pI), negative at pHs above the pI, and positive at pHs below the pI. Irisin has 7 Asp, 11 Glu, 2 His, 8 Lys, and 5 Arg-residues. Consequently, due to more acidic residues present in irisin, the calculated pI value of irisin is 4.9, and the net charge on irisin at physiological pH is ~−5.3. The pH is of utmost importance among the factors that influence the protein conformation and its function. A protein is maximally stable at its isoelectric point (pI) because at pI, its net charge is zero [33,34]. However, any change in

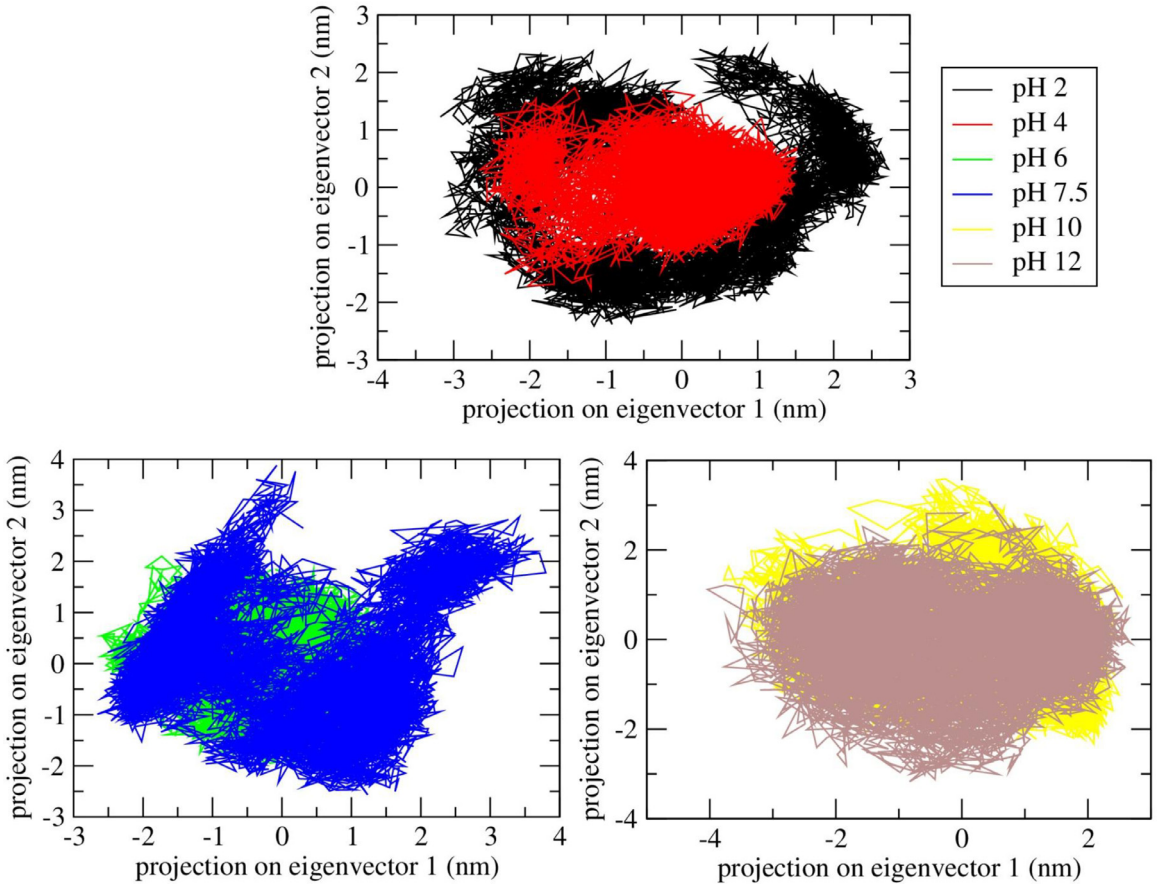

Fig. 6. The 2-D eigen vector projection plot showing the differences between the flexibility of irisin protein in the studied systems.

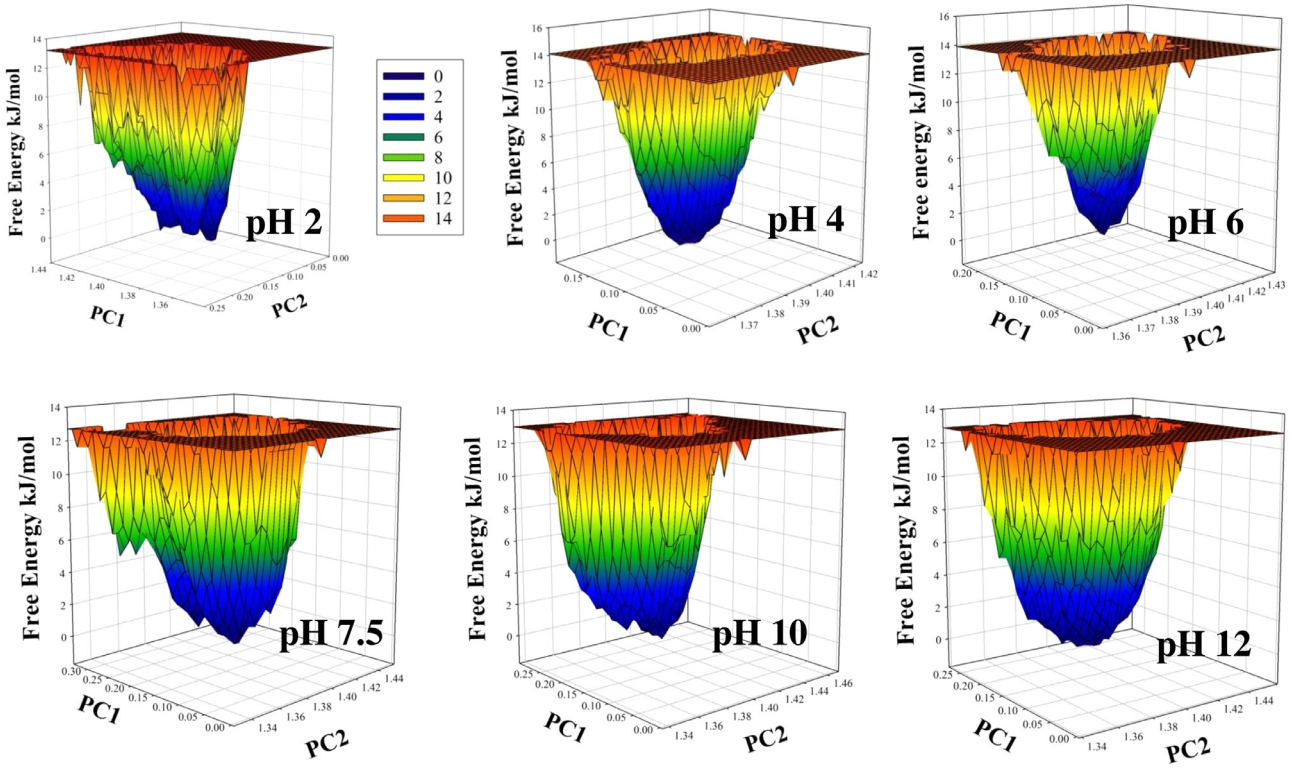

Fig. 7. The plots of free energy landscape observed in the diverse pH conditions during the course of 100 ns MD simulations.

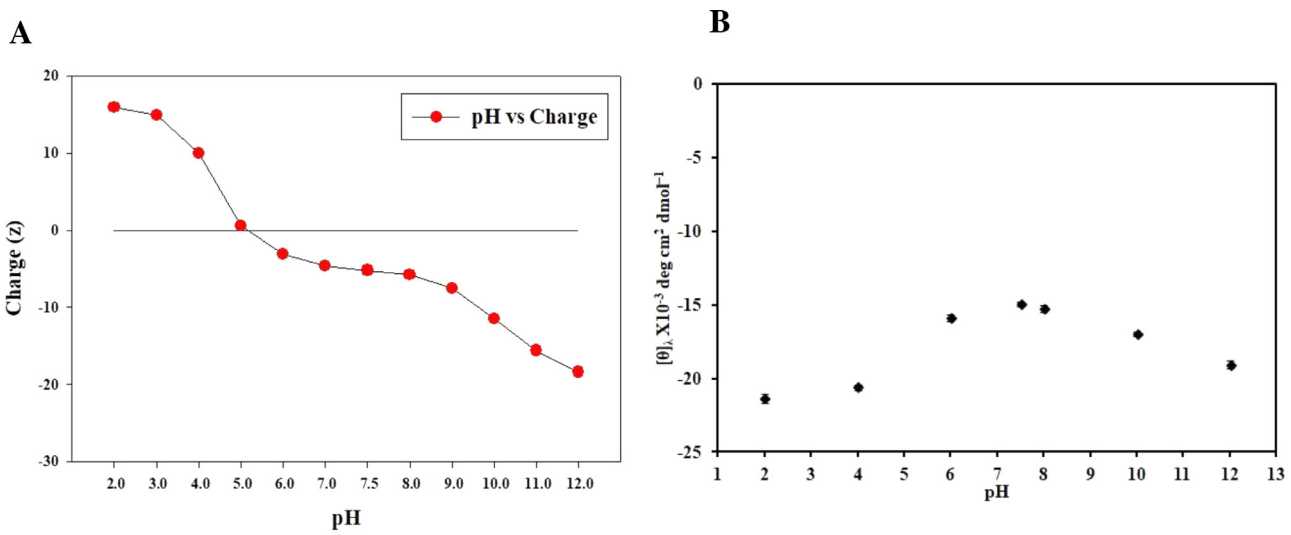

Fig. 8. (A) Graph showing net charge on irisin at different pH. (B) A plot of MRE_{222} v/s pH.

pH may perturb the hydrogen bonds and electrostatic properties that are essential for maintaining stable structure and conformation of protein [35,36]. Therefore, it is evident that pH influences the thermodynamic stability and activity of a protein and suggests that the ionizable groups play an essential role in protein stability [37,38]. Since electrostatic interactions and salt bridges seem to play a fundamental role in protein stability, a deeper knowledge of the pH dependence of the protein stability is important [39].

In 1924, Linderstrom-Lang proposed a model which predicts that proteins should be most stable near their pIs, where their net charge is zero because unfavorable electrostatic interactions due to excess positive or negative charges will be minimized [40]. In Fig. 8A, we have shown the calculated net charge on the irisin protein at different pH values. Fig. 8B depicts the plot of $[\theta]_{222}$ versus pH that shows no significant perturbation of secondary structure in the alkaline pH range (7.0–12.0). However, changes were evident in the acidic pH range with maximum compactness observed at pH 4.0 and so on. According to the CD, fluorescence and *in silico* results, it was predicted that irisin is most stable at pH 4.0 and 6.0, which are nearer pH values to the pI of irisin (i.e., 4.9). The net charge on irisin at pH 4.0 is ∼+8.9 and ∼−3.5 at pH 6.0. As at extreme pH values, i.e., pH 2.0 and 12.0, there is an excess of positive and negative (+15.9 and −17.2) charges, respectively, which might be the reason for increased unfavorable electrostatic interactions causing less protein stability at that pH. So, our results are in agreement with the hypothesis that proteins are mostly stable near their pI.

Although irisin's crystal structure is known, little information is available on its structural and biophysical properties. It is essential to understand the factors which determine the folding process of a linear polypeptide chain into its distinctive three-dimensional structure. The function of any protein is dependent on its 3-D structure and stability. In the surrounding environment of the protein, some crucial factors that govern the structure and stability of protein are pH, ionic strength, and concentration of other co-solvents [41,42]. As protein stability is directly related to its function, pH has a major role in determining protein function in a particular condition. It is well known that interstitial fluid pH plays an important role in maintaining normal cell/body functions. The activity of various enzymes and the binding affinity of hormones and neurotransmitters to their receptors directly depends on the pH of interstitial fluid. Since extracellular fluids have low pH-buffering capacity due to the absence of buffering proteins, over-production of acid metabolites lowers the pH of interstitial fluids, which diminishes the binding affinity of insulin to its receptor, resulting in insulin resistance [43]. Moreover, several epidemiological studies have recently reported the relationship between metabolic acidosis and insulin resistance [44].

Additionally, type 2 diabetes mellitus has been suggested to increase the risk of developing dementia and Alzheimer's disease [45,46]. It was also reported that the pH of interstitial fluid around the hippocampus is lower in type 2 diabetes mellitus model OLETF rats than in normal ones. This observation is suggestive of attenuation of neuronal activity around the hippocampus [47]. So, it can be concluded that lower body fluid pH also causes insulin resistance, leading to the development of synaptic dysfunction and memory impairments related to AD. As mentioned above, irisin is known to have protective action against insulin resistance as well as AD. Since the stable structure and conformation are required for its proper functioning, our motive was to study the effect of pH on irisin stability. If irisin is found to be stable at lower pH, which is the case, it may have implications in therapeutic advancement for the treatment of diabetes and AD.

4. Conclusion

In this study, we have used a multispectroscopic approach coupled with classical MD simulation to illustrate the effect of pH on the structure and stability of irisin. In spectroscopic studies, a remarkable effect of pH on the structure and stability of irisin was observed at acidic pH. It was concluded that both the secondary and tertiary structure is more stable, particularly at pH 4.0 and 6.0. Moreover, a close correlation was also observed during the MD simulation studies. pH-dependent structural studies of irisin will be beneficial to understand the dynamic behavior of irisin and its function in different organelle and regulation of cellular physiology. It was found that the structural property of irisin depends on the pH of the medium. Thus it can provide a molecular basis to understand its function in various conditions. Irisin has an important role in insulin sensitivity and neuroprotection in the case of AD. Since body fluid pH plays an important role in regulating body function, it was observed that lowered pH levels cause insulin resistance via reduced binding affinity of insulin to its receptors. Furthermore, the acidic environment occurring in the brain can also disrupt neuronal function related to AD. Therefore in these conditions, we predict that irisin, which is suggested to be structurally

more stable at lower pH, would be a key factor in developing therapies for metabolic diseases including diabetes and AD.

Authors agreement

The authors confirm that hey have seen the submitted version of the manuscript and have no competing financial interest.

The manuscript is solely submitted to this journal and is not under consideration of publication.

Declaration of Competing Interest

None as per the best knowledge of the authors.

CRediT authorship contribution statement

Rashid Waseem: Conceptualization, Formal analysis, Project administration, Writing – original draft, Writing – review & editing. **Anas Shamsi:** Data curation, Visualization, Methodology, Writing – review & editing. **Mohd Shahbaz:** Visualization, Software. **Tanzeel Khan:** Writing – review & editing. **Syed Naqui Kazim:** Formal analysis, Investigation, Validation. **Faizan Ahmad:** Validation, Data curation. **Md. Imtaiyaz Hassan:** Investigation, Validation. **Asimul Islam:** Formal analysis, Project administration, Writing – review & editing.

Acknowledgments

This work was supported by the grant from the Indian Council of Medical Research ISRM/12/(127)/2020. The authors are grateful to the FIST Program (SR/FST/LSI-541/2012) and Jamia Millia Islamia (a Central University) for providing infrasytructural support to carry out this work. RW acknowledges DST-INSPIRE for INSPIRE Fellowship (IF-180728). AS is thankful to UGC for D.S. Kothari Postdoctoral fellowship ((BSR)/BL/19–20/0119).

Supplementary materials

Supplementary material associated with this article can be found, in the online version, at doi:10.1016/j.molstruc.2021.132141.

References

[1] A. Safdar, M.A. Tarnopolsky, Exosomes as mediators of the systemic adaptations to endurance exercise, Cold Spring Harb. Perspect. Med. 8 (3) (2018) a029827.
[2] P. Boström, J. Wu, M.P. Jedrychowski, A. Korde, L. Ye, J.C. Lo, K.A. Rasbach, E.A. Boström, J.H. Choi, J.Z. Long, A PGC1-α-dependent myokine that drives brown-fat-like development of white fat and thermogenesis, Nature 481 (7382) (2012) 463–468.
[3] M. Gouveia, J. Vella, F. Cafeo, F. Affonso Fonseca, M. Bacci, Association between irisin and major chronic diseases: a review, Eur. Rev. Med. Pharmacol. Sci. 20 (19) (2016) 4072–4077.
[4] M.V. Lourenco, R.L. Frozza, G.B. de Freitas, H. Zhang, G.C. Kincheski, F.C. Ribeiro, R.A. Gonçalves, J.R. Clarke, D. Beckman, A. Staniszewski, Exercise-linked FNDC5/irisin rescues synaptic plasticity and memory defects in Alzheimer's models, Nat. Med. 25 (1) (2019) 165–175.
[5] G. Colaianni, C. Cuscito, T. Mongelli, P. Pignataro, C. Buccoliero, P. Liu, P. Lu, L. Sartini, M. Di Comite, G. Mori, The myokine irisin increases cortical bone mass, Proc. Natl. Acad. Sci. 112 (39) (2015) 12157–12162.
[6] D.J. Li, Y.H. Li, H.B. Yuan, L.F. Qu, P. Wang, The novel exercise-induced hormone irisin protects against neuronal injury via activation of the Akt and ERK1/2 signaling pathways and contributes to the neuroprotection of physical exercise in cerebral ischemia, Metabolism 68 (2017) 31–42.
[7] H. Kim, C.D. Wrann, M. Jedrychowski, S. Vidoni, Y. Kitase, K. Nagano, C. Zhou, J. Chou, V.J.A. Parkman, S.J. Novick, Irisin mediates effects on bone and fat via αV integrin receptors, Cell 175 (7) (2018) 1756–1768 e17.
[8] G.E. Maalouf, D. El Khoury, Exercise-induced irisin, the fat browning myokine, as a potential anticancer agent, J. Obes. (2019) 2019.
[9] X. Provatopoulou, G.P. Georgiou, E. Kalogera, V. Kalles, M.A. Matiatou, I. Papapanagiotou, A. Sagkriotis, G.C. Zografos, A. Gounaris, Serum irisin levels are lower in patients with breast cancer: association with disease diagnosis and tumor characteristics, BMC Cancer 15 (1) (2015) 1–9.
[10] G. Kong, Y. Jiang, X. Sun, Z. Cao, G. Zhang, Z. Zhao, Y. Zhao, Q. Yu, G. Cheng, Irisin reverses the IL-6 induced epithelial-mesenchymal transition in osteosarcoma cell migration and invasion through the STAT3/Snail signaling pathway, Oncol. Rep. 38 (5) (2017) 2647–2656.
[11] A. Roca-Rivada, C. Castelao, L.L. Senin, M.O. Landrove, J. Baltar, A.B. Crujeiras, L.M. Seoane, F.F. Casanueva, M. Pardo, FNDC5/irisin is not only a myokine but also an adipokine, PLoS One 8 (4) (2013) e60563.
[12] M.A. Schumacher, N. Chinnam, T. Ohashi, R.S. Shah, H.P. Erickson, The structure of irisin reveals a novel intersubunit β-sheet fibronectin type III (FNIII) dimer implications for receptor activation, J. Biol. Chem. 288 (47) (2013) 33738–33744.
[13] R. Waseem, A. Shamsi, T. Mohammad, F.A. Alhumaydhi, S.N. Kazim, M.I. Hassan, F. Ahmad, A. Islam, Multispectroscopic and molecular docking insight into elucidating the interaction of irisin with Rivastigmine tartrate: a combinational therapy approach to fight Alzheimer's disease, ACS Omega 6 (11) (2021) 7910–7921.
[14] O. Osman, A. Mahmoud, D. Atta, A. Okasha, M. Ibrahim, Computational notes on the effect of solvation on the electronic properties of glycine, Der Pharm. Chem. 7 (2015) 377–380.
[15] D. Atta, A. Okasha, Single molecule laser spectroscopy, Spectrochim. Acta Part A 135 (2015) 1173–1179.
[16] D. Atta, A.E. Mahmoud, A. Fakhry, Protein structure from the essential amino acids to the 3D structure, Biointerface Res. Appl. Chem. 9 (1) (2019) 3817–3824.
[17] A.M. Galal, D. Atta, A. Abouelsayed, M.A. Ibrahim, A.G. Hanna, Configuration and molecular structure of 5-chloro-N-(4-sulfamoylbenzyl) salicylamide derivatives, Spectrochim. Acta Part A 214 (2019) 476–486.
[18] M.A. El-Sheikh, A. Al-Enezy, F. El-Enezy, D. Ashammri, W. Alrowili, A novel method for the preparation of conductive methyl cellulose-silver nanoparticles-polyaniline-nanocomposite, Egypt. J. Chem. 63 (9) (2020) 8–9.
[19] R. Waseem, S. Anwar, S. Khan, A. Shamsi, M. Hassan, F. Anjum, A. Shafie, A. Islam, D.K. Yadav, MAP/Microtubule affinity regulating kinase 4 inhibitory potential of irisin: a new therapeutic strategy to combat cancer and Alzheimer's disease, Int. J. Mol. Sci. 22 (20) (2021) 10986.
[20] N.J. Greenfield, Using circular dichroism spectra to estimate protein secondary structure, Nat. Protoc. 1 (6) (2006) 2876.
[21] J.T. Yang, C.S.C. Wu, H.M. Martinez, [11]Calculation of protein conformation from circular dichroism, Meth. Enzymol. 130 (1986) 208–269.
[22] E. Alexov, E.L. Mehler, N. Baker, A.M. Baptista, Y. Huang, F. Milletti, J.E. Nielsen, D. Farrell, T. Carstensen, M.H.M. Olsson, J.K. Shen, J. Warwicker, S. Williams, J.M. Word, Progress in the prediction of pKa values in proteins, Proteins 79 (12) (2011) 3260–3275.
[23] C.A. Fuzo, L. Degreve, The pH dependence of flavivirus envelope protein structure: insights from molecular dynamics simulations, J. Biomol. Struct. Dyn. 32 (10) (2014) 1563–1574.
[24] J.C. Gordon, J.B. Myers, T. Folta, V. Shoja, L.S. Heath, A. Onufriev, H++: a server for estimating pKas and adding missing hydrogens to macromolecules, Nucl. Acids Res. 33 (Web Server issue) (2005) W368–W371.
[25] S. Pronk, S. Pall, R. Schulz, P. Larsson, P. Bjelkmar, R. Apostolov, M.R. Shirts, J.C. Smith, P.M. Kasson, D. van der Spoel, B. Hess, E. Lindahl, GROMACS 4.5: a high-throughput and highly parallel open source molecular simulation toolkit, Bioinformatics 29 (7) (2013) 845–854.
[26] V. Hornak, R. Abel, A. Okur, B. Strockbine, A. Roitberg, C. Simmerling, Comparison of multiple Amber force fields and development of improved protein backbone parameters, Proteins 65 (3) (2006) 712–725.
[27] J. Zielkiewicz, Structural properties of water: comparison of the SPC, SPCE, TIP4P, and TIP5P models of water, J. Chem. Phys. 123 (10) (2005) 104501.
[28] J. Kaminchik, N. Bashan, D. Pinchasi, B. Amit, N. Sarver, M. Johnston, M. Fischer, Z. Yavin, M. Gorecki, A. Panet, Expression and biochemical characterization of human immunodeficiency virus type 1 nef gene product, J. Virol. 64 (7) (1990) 3447–3454.
[29] M.R. Eftink, C.A. Ghiron, Fluorescence quenching studies with proteins, Anal. Biochem. 114 (2) (1981) 199–227.
[30] L.A. Munishkina, A.L. Fink, Fluorescence as a method to reveal structures and membrane-interactions of amyloidogenic proteins, Biochim. Biophys. Acta 1768 (8) (2007) 1862–1885 (BBA)-Biomembr..
[31] A.S. Yang, B. Honig, Free energy determinants of secondary structure formation: II. Antiparallel β-sheets, J. Mol. Biol. 252 (3) (1995) 366–376.
[32] C. Tanford, The interpretation of hydrogen ion titration curves of proteins, Adv. Protein Chem. 17 (1963) 69–165.
[33] M.K.A. Khan, U. Das, M.H. Rahaman, M.I. Hassan, A. Srinivasan, T.P. Singh, F. Ahmad, A single mutation induces molten globule formation and a drastic destabilization of wild-type cytochrome c at pH 6.0, JBIC J. Biol. Inorg. Chem. 14 (5) (2009) 751–760.
[34] M.K.A. Khan, M.H. Rahaman, M.I. Hassan, T.P. Singh, A.A. Moosavi-Movahedi, F. Ahmad, Conformational and thermodynamic characterization of the premolten globule state occurring during unfolding of the molten globule state of cytochrome c, JBIC J. Biol. Inorg. Chem. 15 (8) (2010) 1319–1329.
[35] S. Berne, K. Sepčić, G. Anderluh, T. Turk, P. Macek, N.P. Ulrih, Effect of pH on the pore forming activity and conformational stability of ostreolysin, a lipid raft-binding protein from the edible mushroom Pleurotus ostreatus, Biochemistry 44 (33) (2005) 11137–11147.
[36] N.A. Kim, I.B. An, D.G. Lim, J.Y. Lim, S.Y. Lee, W.S. Shim, N.G. Kang, S.H. Jeong, Effects of pH and buffer concentration on the thermal stability of etanercept using DSC and DLS, Biol. Pharm. Bull. 37 (5) (2014) 808–816.

[37] B. Honig, A. Nicholls, Classical electrostatics in biology and chemistry, Science 268 (5214) (1995) 1144–1149.
[38] D. Kishore, S. Kundu, A.M. Kayastha, Thermal, chemical and pH induced denaturation of a multimeric β-galactosidase reveals multiple unfolding pathways, PLoS One 7 (11) (2012) e50380.
[39] J.H. Missimer, M.O. Steinmetz, R. Baron, F.K. Winkler, R.A. Kammerer, X. Daura, W.F. Van Gunsteren, Configurational entropy elucidates the role of salt-bridge networks in protein thermostability, Protein Sci. 16 (7) (2007) 1349–1359.
[40] K. Linderstrøm-Lang, On the ionization of proteins, CR Trav. Lab. Carlsberg 15 (7) (1924) 1–29.
[41] D. Idrees, M. Shahbaaz, K. Bisetty, A. Islam, F. Ahmad, M.I. Hassan, Effect of pH on structure, function, and stability of mitochondrial carbonic anhydrase VA, J. Biomol. Struct. Dyn. 35 (2) (2017) 449–461.
[42] H. Naz, M. Shahbaaz, K. Bisetty, A. Islam, F. Ahmad, M.I. Hassan, Effect of pH on the structure, function, and stability of human calcium/calmodulin-dependent protein kinase IV: combined spectroscopic and MD simulation studies, Biochem. Cell. Biol. 94 (3) (2016) 221–228.
[43] H. Hayata, H. Miyazaki, N. Niisato, N. Yokoyama, Y. Marunaka, Lowered extracellular pH is involved in the pathogenesis of skeletal muscle insulin resistance, Biochem. Biophys. Res. Commun. 445 (1) (2014) 170–174.
[44] G. Souto, C. Donapetry, J. Calvino, M.M. Adeva, Metabolic acidosis-induced insulin resistance and cardiovascular risk, Metab. Syndr. Relat. Disord. 9 (4) (2011) 247–253.
[45] R. Waseem, A. Shamsi, S. Kazim, A. Islam, An insight into mitochondrial dysfunction and its implications in neurological diseases, Curr. Drug Targets (2020) (Print).
[46] M. Madmoli, Y. Modheji, A. Rafi, R. Feyzi, P. Darabiyan, A. AfsharNia, Diabetes and its predictive role in the incidence of Alzheimer's disease, Med. Sci. 23 (95) (2019) 30–34.
[47] Y. Marunaka, Roles of interstitial fluid pH in diabetes mellitus: glycolysis and mitochondrial function, World J. Diabetes 6 (1) (2015) 125.